Cellular & Molecular Biology
Cell. Mol. Biol. 2015; 61 (2): 86-93
Published online May 28, 2015 (http://www.cellmolbiol.com)
Received on April 19, 2015, Accepted on May 18, 2015.
doi : 10.14715/cmb/2015.61.2.15

Investigation of cell aggregation on the substrate of a parallel-plate flow chamber

F. Bai[1], C. Dong[3], C. Cao[2] and R. Sun[1]

[1] Department of Engineering Mechanics, Shanghai Jiao Tong University, Shanghai 200240, China
[2] School of Life Science & Biotechnology, Shanghai Jiao Tong University, Shanghai 200240, China
[3] Department of Bioengineering, The Pennsylvania State University, 233 Hallowell Building, University Park, PA 16802, USA

Corresponding author: R. Sun, Department of Engineering Mechanics, Shanghai Jiao Tong University, Shanghai 200240, China. E-mail: drr-sun@sjtu.edu.cn

Abstract

Adhesion of tumor cells (TCs) to polymorphonuclear neutrophils (PMNs) tethered on a monolayer of vascular endothelial cells (ECs) in shear flows is investigated theoretically. Both TC-PMN and PMN-EC aggregations are modeled using the population balance equations (PBEs). Parameters in the model obtained by curve fitting show that an increase of shear rate or viscosity will suppress the formation of aggregates and promote the breakage of them. Analysis on the collision frequency suggests that the averaged encounter duration is affected by viscosity. Based on the model, a nonlinear connection between the number of migrated TCs and the concentration of PMNs in the flow near the substrate is presented.

Key words: Tumor cells, PMNs, Cell adhesion, Population balance equations, Probability prediction.

Introduction

Tumor cells are often observed moving with blood flows, occasionally adhering to a blood vessel wall and migrating through it. So understanding of adhesion of TCs is important to further medical treatment of cancer. In recent years, some investigators have pointed out that polymorphonuclear neutrophils (PMNs) would assist a few kinds of tumor cells to extravasate from the blood vessels to the surrounding tissues (1-5) through PMN-TC aggregation. It is usually thought that two factors influence the PMN-TC aggregation: one is the hydrodynamic factor (shear rate and viscosity) which affects the approach of TCs to PMNs and deformation of these cells, and the other relates to the properties of receptors and ligands on surfaces of PMNs and TCs which may form intercellular bonds (6-10).

To investigate the PMN-TC aggregation in vitro, TCs and PMNs are usually released in a shear flow in order to explore how PMNs help TCs rest on walls of the blood vessels. Liang et al. (6) designed such a device so as to explore the effect of shear flows on the PMN-facilitated adhesion of melanoma cells (MCs) to the EC monolayer, and found that this process was modulated by the shear rate rather than the shear stress. For comparison with the previous investigations, Liang et al. (7) also used this device to investigate the aggregation of PMNs and MCs in the absence of ECs. Slattery et al. (2) in their experiments on migrated cells came to the same conclusion that the number of migrated MCs was mainly influenced by the shear rate. Besides, the cone plate viscometer which could create a constant shear rate was also frequently used in various researches (11-14) so as to explore the aggregation of cells in different shear flows.

To explain experimental results and make reliable predictions, the population balance equations (PBEs) introduced by Smoluchowski (15, 16) are usually employed and expressed as

$$\frac{dC_i}{dt}=\frac{1}{2}\sum_{j=1}^{i-1}k_{i-j,j}C_{i-j}C_j-\sum_{j=1}^{N-i}k_{i,j}C_iC_j-\sum_{j=1}^{i-1}b_{j,i}C_i+\sum_{j=i+1}^{N}b_{i,j}C_j \quad (i=1,2...N), \quad (1)$$

where C_i is the concentration of such aggregates that each one of them is composed of i particles and N the maximum number of particles an aggregate may contain. Here $k_{i,j}$ denotes the rate of formation of a new aggregate from two aggregates respectively composed of i and j particles, and $b_{i,j}$ the rate of breakage of an aggregate made up of i particles into a smaller one of i particles. In the earlier researches, the PBEs were used to model aggregations of just one kind of cell, such as platelets (13, 14) or neutrophils (12). Recently, Wang et al. (17) and Ma et al. (18) tried to use the PBEs to model a heterotypic-cell aggregation of PMNs and TCs.

However, for the problem of the aggregation of PMNs and TCs on the EC monolayer in a shear flow, the main difficulty in using the PBEs is how to determine the formation and breakage coefficients, $k_{i,j}$ and $b_{i,j}$. As mentioned in Ref. (18), the formation coefficient equals the product of the collision frequency (number of collisions per unit time per unit concentration) and the adhesion efficiency (probability of forming a new heterotypic-cell aggregate in a collision). The collision frequency is determined hydrodynamically by shapes of tethered PMNs and velocities of TCs in the shear flow near a wall, and the adhesion efficiency is related to the bonds formed between these two cells. According to Ref. (11), equations for bond kinetics are

$$\frac{dp_n}{dt}=A_cm_rm_lk_f^{(n)}p_{n-1}-\left(A_cm_rm_lk_f^{(n+1)}+nk_r^{(n)}\right)p_n+(n+1)k_r^{(n+1)}p_{n+1}\ (n=1,2...), \quad (2)$$

where n denotes the probability of forming n bonds at time t when two cells keep in touch, m_r and m_l the number of receptors and ligands per unit area, respectively and A_c the contact area. Here $k_f^{(n)}$ is the forward action rate of forming n bonds from $(n-1)$ bonds, and

$k_r^{(n)}$ the reverse action rate of forming n bonds from $(n+1)$ bonds. Equation (2) is valid on the assumption that the number of formed bonds is much smaller than that of receptors or ligands in the contact area. Fu et al. (19) used an extended version of Eq. (2) to study cell aggregation in a cone plate viscometer, specifying that $k_f^{(n)}$ was constant for any n and thus expressed as k_f. Hence in Ref. (19) the adhesion efficiency was calculated as

$$\varepsilon = A_c m_r m_l k_f \overline{\tau}\,, \tag{3}$$

where ε denotes the adhesion efficiency and $\overline{\tau}$ the averaged encounter duration. According to Ref. (20), $\overline{\tau}$ is calculated as

$$\overline{\tau} = \frac{\pi\left(r_e + 1/r_e\right)}{G\left(r_e+1\right)}, \tag{4}$$

where G denotes shear rate, and $\overline{\tau}$ the equivalent aspect ratio of a two-cell doublet which behaves like an ellipsoid in shear flows. Eq. (4) is valid for such a doublet composed of two rigid cell spheres in an unbounded shear flow, and indicates that $\overline{\tau}$ is inversely proportional to the shear rate. However, for the case of a doublet composed of two deformable cells in a bounded shear flow, the relationship between $\overline{\tau}$ and G is not clear. Moreover, it is unknown whether other parameters such as viscosity also affect $\overline{\tau}$.

To assess the breakage coefficient $b_{i,j}$, some investigators (21,22) suggested an expression to describe the decomposition of colloidal aggregations, which was later adopted to model the decomposition of platelet aggregations (13). In these investigations, $b_{i,j}$ takes the form of $g(j)\gamma(j)p_s(j,i)$. For an aggregate composed of j cells, $g(j)$ is a rate of breakage of the aggregate, $\gamma(j)$ the number of daughter fragments of the aggregate, and $p_s(j,i)$ the ratio of the number of fragments composed of i cells to that of all fragments. Neelamegham et al. (12) mentioned that $g(j)$ depended on the shear rate. A reasonable relationship between $b_{i,j}$ and the shear rate was given by Spicer (23) and confirmed by Serra et al. (24) for latex particles. However, for the case of breakage of PMN-MC aggregates, it is difficult to determine $b_{i,j}$ because forces exerted on each bond and contact areas between the two cells are unknown.

In the present study, a modified model is proposed for adhesion of TCs to PMNs tethered on an EC monolayer covering the substrate of a parallel plate flow chamber. To do this, all the possible sorts of formation and breakage of the two heterotypic cell aggregates on the monolayer in a blood flow are specified, and two population balance equations for PMN-TC doublets and PMN monomers tethered on the monolayer are established. Based on the available experiments, where melanoma cells were used as TCs (6), parameters at different shear rates and viscosities in the model are obtained by curve fitting and the averaged encounter duration is analyzed. Considering the connections between the parameters in the model and the concentrations of TCs and PMNs, a formula used to predict the numbers of migrated TCs at different concentrations of PMNs is presented.

Theoretical analysis

The aggregations of the three heterotypic cells are schematically shown in Figs. 1(A). In the figure, a suspension of deformable PMNs and TCs is injected into a parallel plate flow chamber whose substrate is coated over an EC monolayer. In the previous experiments (6), the length, width and height of the chamber are 800μm, 600μm and 127μm, respectively. The concentrations of PMNs and TCs are all 1×10^6mL^{-1}. The shear rate near the substrate can be adjusted by changing the flux of the fluid at the inlet. The viscosity of the fluid can be modified by varying the amount of dextran. The ECs used in these experiments can capture the nearby flowing PMNs, because the E-selectins expressed on their surfaces are able to form bonds with the sLe^X (Sialyl Lewis X, a kind of sialylated molecules) on the surfaces of PMNs as shown in Fig. 1(B). Besides, ICAM-1 (intercellular adhesion molecule-1) on the surfaces of ECs and β_2-integrins on the surfaces of PMNs will also form bonds and promote the capture of PMNs by ECs (6, 18). Melanoma cells are used as TCs which also have ICAM-1 on their surfaces, so they can adhere to PMNs. However, melanoma cells cannot directly adhere to ECs because there are neither sLe^X nor β_2-integrins on their surfaces. Thus, there appear PMN monomers and PMN-TC doublets on the EC monolayer in these experiments, which are shown in Fig. 2.

It should be mentioned that in these experiments, the possibility for a PMN to tether on the substrate is low and the possibility for a TC to adhere to a tethered PMN is even lower because only bonds composed of ICAM-1 and β_2-integrin will lead to such adhesion. So only a small number of PMN-TC doublets can be observed, and aggregates on the substrate containing more than two cells are hardly seen (18). Thus the number of these aggregates can be ignored compared to that of PMN-TC doublets and the following five kinds of cell aggregations and breakages on the EC monolayer are to be modeled:

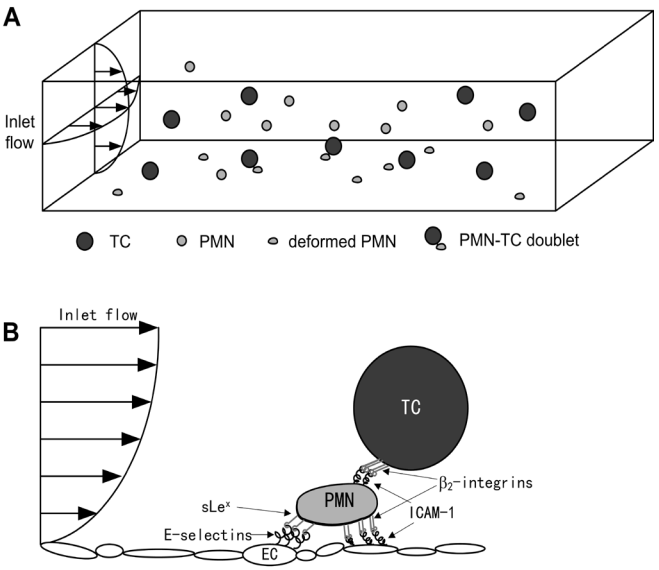

Figure 1. Cell aggregation in a parallel plate flow chamber. (A) A suspension of PMNs and TCs is injected into a parallel plate flow chamber. (B) A schematic diagram is drawn for a PMN-TC doublet linked to the EC monolayer covering the substrate of the chamber.

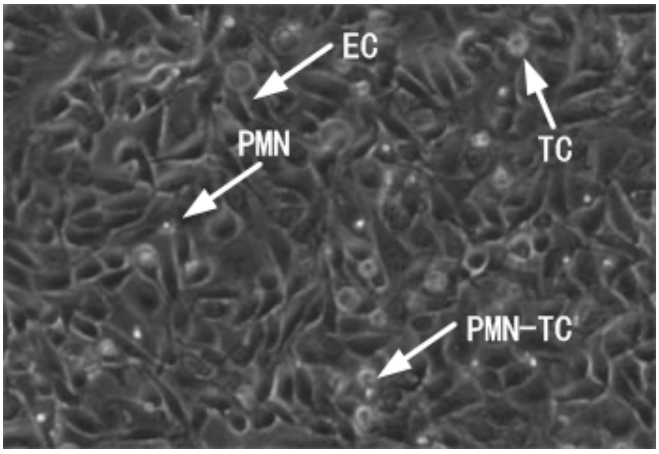

Figure 2. A top view of a part of the substrate of parallel-plate flow chamber. The small white particles are PMNs and the slightly dark spherical particles are TCs. Those cells with arbitrary shapes on the bottom are ECs. A PMN-TC doublet is also seen. The flow is from left to right.

(1) PMNs colliding with the EC monolayer may be tethered on it,
(2) A TC colliding with a tethered PMN can form a PMN-TC doublet,
(3) Breakage of bonds on the surface of a PMN-TC doublet makes the TC flee away and the PMN stay alone on the monolayer,
(4) The PMN-TC doublet leaves the substrate due to the breakage of bonds between the doublet and the monolayer,
(5) The PMN leaves the substrate because of bond breakage between the PMN and the monolayer.

To give a quantitative description of these five kinds of adhesion and breakage phenomena, the numbers of tethered PMN monomers and PMN-TC doublets per unit area of the EC monolayer, denoted by N_P and N_{PT} respectively, need to be determined. For convenience, case (2) is discussed first. It indicates that a tethered PMN can capture a moving TC in the flow near the wall, which will increase the number of PMN-TC doublets and decrease that of the tethered PMN monomers at the same time. As Fig. 3 shows, the collision frequency f_{PT} between a tethered PMN and migrating TCs can be calculated by

$$f_{PT} = \int_{\Omega, \vec{v}\cdot\vec{n}\le 0} C_T \left|\vec{v}\cdot\vec{n}\right| dS, \tag{5}$$

where C_T is a concentration (number per unit volume) of TCs near the monolayer, $\vec{v}$ the average velocity of TCs, $\vec{n}$ the envelope surface of the tethered PMN and $\vec{n}$ the outer normal vector of Ω. C_T is regarded as a constant in the paper. In reality, the capture of TCs by tethered PMNs will decrease C_T, but such a decrease can be ignored because the flowing TCs are much more than the tethered TCs. After a TC collides with a tethered PMN, how many bonds will form between them is stochastic rather than deterministic (11, 25). Let ε_{PT} denote the adhesion efficiency for the two cells, and then the rate of change of the number of PMN-TC doublets formed per unit area is $f_{PT}\varepsilon_{PT}N_P$. Accordingly, the rate of change of the number of tethered PMN monomers is $-f_{PT}\varepsilon_{PT}N_P$ per unit area. Thus, the formation coefficient k_{PT} of PMN-TC doublets is

$$k_{PT} = f_{PT}\varepsilon_{PT}, \tag{6}$$

Obviously, k_{PT} varies linearly with C_T according to Eq. (5).

To describe case (1), it should be made clear that in the near-wall region of a shear flow, tethered PMNs and PMN-TC doublets on the monolayer would influence tethering of new PMN comers due to hydrodynamic effects. Fig. 4 shows that some ECs close to a tethered PMN and PMN-TC doublet cannot be touched by the moving PMNs. Denoting the number of these ECs as the sum of αN_P and $\beta N_{PT}$where α and β are two hydrodynamic influence coefficients, the rate of change of the number of tethered PMNs per unit area only due to collisions of moving PMNs with the monolayer, T_f, is

$$T_f = k_{PE}\left(N_E^0 - \alpha N_P - \beta N_{PT}\right), \tag{7}$$

where N_E^0 is the number of ECs per unit area of the substrate. k_{PE} is the formation coefficient of tethered PMNs and directly proportional to C_P, the concentration of PMNs in the flow near the substrate. Here C_P is also regarded as a constant due to the reason similar to N_P.

Case (3) is about the breakage of PMN-TC doublets, which causes an increase of and a decrease of N_{PT}. Physiologically, when the bond force between a PMN and a TC in a doublet are not great enough to hold the two cells together, the hydrodynamic loads induced by the shear flow will drive the TC away from the PMN. According to the population balance equations given by Smoluchowski (15), the rate of change of the number

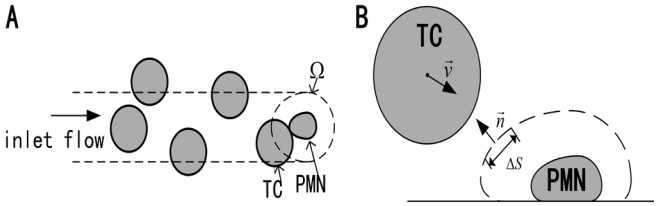

Figure 3. TCs colliding with a PMN. (A) top view, (B) side view.

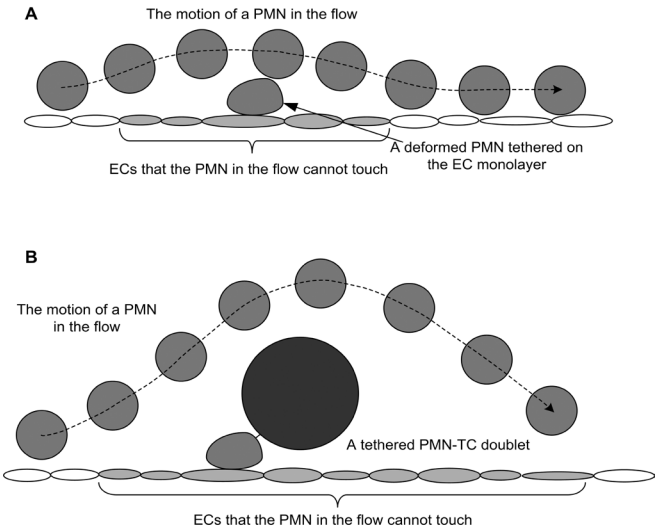

Figure 4. A moving PMN in the shear flow cannot touch influenced EC areas. (A) around a tethered PMN, (B) around a tethered PMN-TC doublet.

of breakage of PMN-TC doublets per unit area can be expressed as $b_{PT}N_{PT}$, where b_{PT} is a breakage coefficient. In cases (4) and (5), similar to case (3), the rate of change of the number of detached PMN-TC doublets and PMN monomers from the monolayer per unit area can be respectively expressed as $b_{PT-E}N_{PT}$ and $b_{PE}N_P$, where b_{PT-E} and b_{PE} are the corresponding breakage coefficients. The breakage of bonds between cells is determined by properties of adhesion molecules on these cells and the shear-rate conditions induced by the flow, so b_{PT}, b_{PT-E} and b_{PE} are not influenced by C_T or C_P. Based on the above analysis on adhesion and breakage of the cell aggregates, a set of differential equations of N_{PT} and N_P are established as follows

$$\frac{dN_{PT}}{dt} = k_{PT}N_P - b_{PT}N_{PT} - b_{PT-E}N_{PT}, \tag{8}$$

$$\frac{dN_P}{dt} = k_{PE}\left[N_E^0 - \alpha N_P - \beta N_{PT}\right] - b_{PE}N_P + b_{PT}N_{PT} - k_{PT}N_P, \tag{9}$$

Eqs. (8) and (9) can be changed into an expression in matrix form as

$$\frac{d}{dt}\begin{bmatrix} N_{PT} \\ N_P \end{bmatrix} = \begin{bmatrix} A & B \\ C & D \end{bmatrix}\begin{bmatrix} N_{PT} \\ N_P \end{bmatrix} + \begin{bmatrix} 0 \\ F \end{bmatrix}, \tag{10}$$

where $A = -\left(b_{PT} + b_{PT-E}\right)$, $B = k_{PT}$, $C = b_{PT} - \beta k_{PE}$, $D = -\left(\alpha k_{PE} + k_{PT} + b_{PE}\right)$ and $F = k_{PE}N_E^0$. Since there are no PMNs and PMN-TC doublets on the monolayer at the beginning of every experiment, the initial conditions of Eq. (10) becomes

$$\left.\begin{bmatrix} N_{PT} \\ N_P \end{bmatrix}\right|_{t=0} = \begin{bmatrix} 0 \\ 0 \end{bmatrix}, \tag{11}$$

Thus N_{PT} and N_P can be derived,

$$N_{PT} = \frac{BF}{\lambda_2 - \lambda_1}\left[\frac{1-e^{\lambda_1 t}}{\lambda_1} - \frac{1-e^{\lambda_2 t}}{\lambda_2}\right], \tag{12}$$

$$N_P = \frac{BF}{\lambda_2 - \lambda_1}\left[\frac{\lambda_1 - A}{B}\frac{1-e^{\lambda_1 t}}{\lambda_1} - \frac{\lambda_2 - A}{B}\frac{1-e^{\lambda_2 t}}{\lambda_2}\right], \tag{13}$$

where λ_1 and λ_2 are the two eigenvalues of matrix $\begin{bmatrix} A & B \\ C & D \end{bmatrix}$.

It is noted that if the aggregation and the breakage maintain a balance, both N_{PT} and N_P become constant, and thus values of λ_1 and λ_2 should be negative.

Substitution of Eqs. (12) and (13) into Eq. (7) yields

$$T_f = k_{PE}\left\{N_E^0 - \frac{BF}{\lambda_2 - \lambda_1}\left[\left(\alpha\frac{\lambda_1 - A}{B} + \beta\right)\frac{1-e^{\lambda_1 t}}{\lambda_1} - \left(\alpha\frac{\lambda_2 - A}{B} + \beta\right)\frac{1-e^{\lambda_2 t}}{\lambda_2}\right]\right\}, \tag{14}$$

Eq. (14) shows that T_f is a function of time in contrast to that in Ref. (18) which regards T_f as an empirical constant, and explains how tethered PMNs and PMN-TC doublets on the monolayer affect tethering of new PMN comers due to hydrodynamic interactions.

Aggregation percentage α_P of tethered PMN-TC doublets is usually defined as

$$\alpha_P = \frac{N_{PT}}{N_{PT} + N_P}, \tag{15}$$

Hence substituting Eqs. (12) and (13) into Eq. (15) gives

$$\alpha_P = \frac{\dfrac{1-e^{\lambda_1 t}}{\lambda_1} - \dfrac{1-e^{\lambda_2 t}}{\lambda_2}}{\left(\dfrac{\lambda_1 - A}{B} + 1\right)\dfrac{1-e^{\lambda_1 t}}{\lambda_1} - \left(\dfrac{\lambda_2 - A}{B} + 1\right)\dfrac{1-e^{\lambda_2 t}}{\lambda_2}}, \tag{16}$$

If values of λ_1 and λ_2 are negative, as $t \to \infty$ α_P becomes,

$$\left.\alpha_P\right|_{t=\infty} = \frac{B}{B - A} = \frac{k_{PT}}{k_{PT} + b_{PT} + b_{PT-E}}, \tag{17}$$

The discussion on formation and breakage coefficients shows that $\left.\alpha_P\right|_{t=\infty}$ is only affected by C_T.

Results and Discussion

Curve fitting of aggregation percentage α_P

The experimental data in Ref. (18) are applied to curve fitting so as to determine the parameters in Eq. (16) using the Levenberg-Marquart method. Table 1 gives the parameters obtained by curve fitting at different shear rates and viscosities and the corresponding values of R^2. For a data set containing n values, let y_i $(i = 1, 2, ..., n)$ denote its members and f_i $(i = 1, 2, ..., n)$ the values predicted by a model, and then R^2 from the data set is defined as

$$R^2 = 1 - \frac{\sum_{i=1}^{n}\left(y_i - f_i\right)^2}{\sum_{i=1}^{n}\left(y_i - \frac{1}{n}\sum_{i=1}^{n} y_i\right)^2}, \tag{18}$$

As the value of R^2 is near 1, it means that the curve fits

Table 1. Parameters obtained by curve fitting under different shear rates and viscosities.

G(s^{-1})	μ(cP)	A(s^{-1})	B(s^{-1})	λ_1(s^{-1})	λ_2(s^{-1})	R^2
62.5	1	-0.01317	0.002266	-0.03041	-0.08287	0.987
62.5	2	-0.0179	0.001587	-0.02119	-0.08138	0.974
62.5	3.2	-0.01977	0.000462	-0.01794	-0.05242	0.987
100	1	-0.01602	0.000974	-0.02432	-0.0842	0.980
100	2	-0.02332	0.000725	-0.01962	-0.04044	0.988
100	3.2	-0.02745	9.92E-05	-0.01334	-0.02742	0.982
200	1	-0.02681	0.000649	-0.02113	-0.02068	0.973
200	2	-0.03243	0.00015	-0.01406	-0.02968	0.983
200	3.2	-0.03902	0.000104	-0.01545	-0.03981	0.988

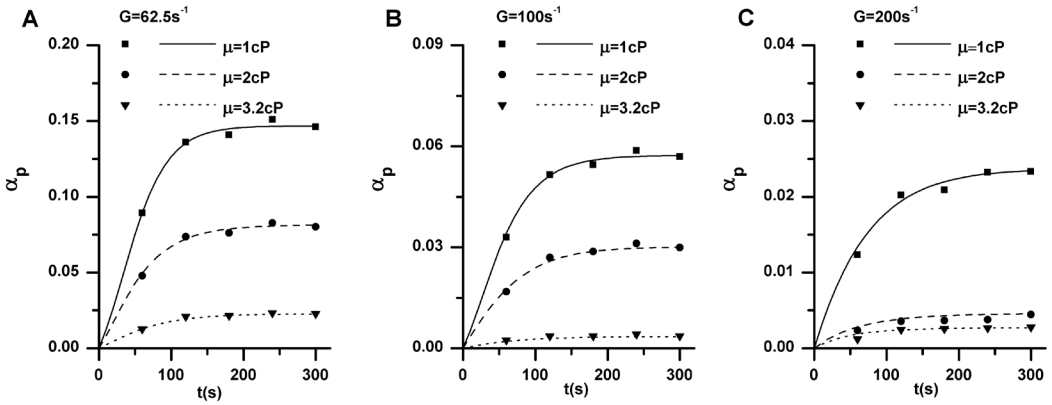

Figure 5. Results of curve fitting. The lines are plotted using theoretical formula (16) with parameters taking their best-fit values and dots denote experimental data. μ is viscosity.

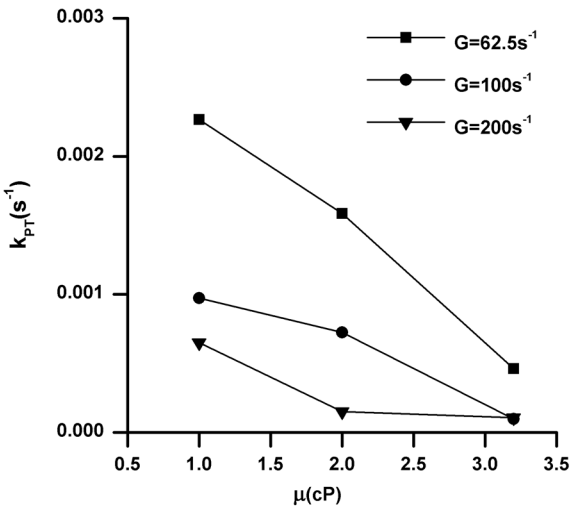

Figure 6. Best-fit values of k_{PT} .

the data well.

Note from Table 1 that values of A in the third column are negative consistent with the expression $A=-\left(b_{PT}+b_{PT-E}\right)$ because b_{PT} and b_{PT-E} are positive. A is at most one tenth of the absolute value of for every case. The reason is that α_p from available experimental data in Ref. (18) is at most of an order of 10^{-1}, and then based on Eq. (17)

$$\alpha_p \approx \frac{B}{B-A} \approx \frac{B}{-A} \text{ and } B \approx \alpha_p |A|, \tag{19}$$

It means that the formation coefficient is much smaller than the breakage one in real shear flows. Table 1 also shows that λ_1 and λ_2 are negative, and it implies that both N_P and N_{PT} will approach constants with time and the aggregation will balance the breakage.

Fitted curves and the experimental data are plotted in Fig. 5. Note that the predictions made by the present model agree well with those experimental data in Ref. (18) if appropriate values of parameters are chosen. It indicates that the model can better describe these biomechanical experiments on cell aggregation. Besides, all fitted curves become flat when *t* approaches 300s, indicating a balance between formation and breakage of aggregates. Fig. 6 shows that k_{PT} varies inversely with shear rate or viscosity. This indicates that the formation of PMN-TC doublets is restrained at high shear rates and viscosities.

Fig. 7 presents that $b_{PT}+b_{PT-E}$ increases monotonically with shear rate or viscosity, and it suggests that the breakage of aggregates due to the rupture of bonds is promoted by the shear rate or viscosity. This conclusion can be explained by Bell Model (26) which proposes that the rate of bond rupture increases with forces exerted on bonds and the hydrodynamic effect that larger shear rates or viscosities elevate the shear forces that wash away the captured TCs and tethered doublets.

Analysis of collision frequency f_{PT}

According to Eq. (6), the collision frequency is calculated by

$$f_{PT}=\frac{k_{PT}}{\varepsilon_{PT}}, \tag{20}$$

where k_{PT} is obtained from the curve fitting and ε_{PT} from experiments in Ref. (6). Fig. 8 shows that f_{PT} diminishes with shear rate or viscosity except for the case of $\mu=3.2cP$. The decrease of f_{PT} in most cases should be attributed to smaller front face areas of tethered PMNs because the hydrodynamic loads increase with shear rate or viscosity which will reduce the heights of those PMNs. f_{PT} increases with the shear rate from $100s^{-1}$ to $200s^{-1}$ and the viscosity of $3.2cP$ because of

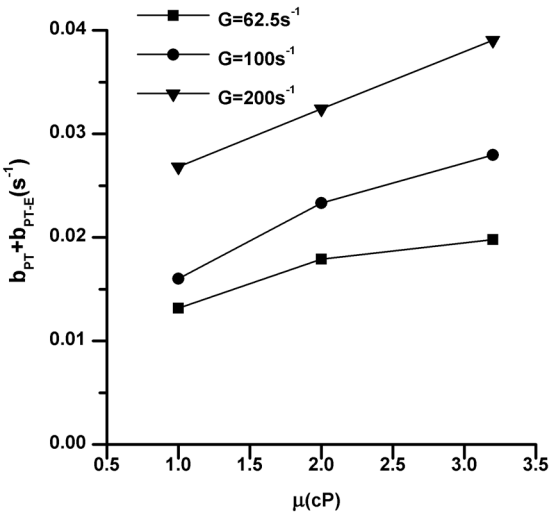

Figure 7. Best-fit values of $\left(b_{PT}+b_{PT-E}\right)$.

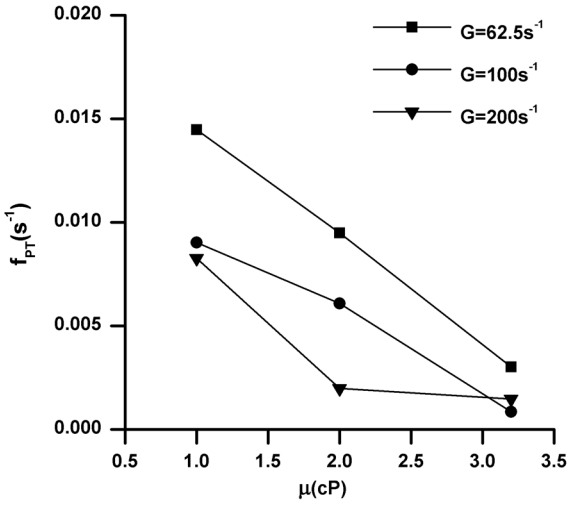

Figure 8. Collision frequencies under different shear rates and viscosities.

higher velocities of moving TCs and less deformed tethered PMNs.

In view of Eq. (3), the averaged encounter duration denoted by $\overline{\tau}$ can be expressed as

$$\overline{\tau} = \frac{\varepsilon_{PT}}{A_c m_r m_l k_f}, \quad A_c \tag{21}$$

The variation of with viscosity at a constant shear rate in Fig. 8 implies the change of A_c due to evident deformations of tethered PMNs. Therefore according to Eq. (21), the averaged encounter duration for collision between two cells when at least one of them is deformable is influenced by viscosity. It is different from Ref. (11) and Ref. (19) since they model cells as hard spheres and regard A_c as a constant.

Migration of TCs under different concentration of PMNs

As a practical example, the number of migrated TCs per unit area denoted as n_M is calculated to explain the previous experiments of migration of TCs under different concentrations of PMNs (2). Although its parallel-plate flow chamber is different in size from that in the adhesion experiments (6), the current model is applicable because it only deals with quantities per unit area such as N_P and N_{PT}. The TCs used in the migration experiments are C8161 cells which also express ICAM-1 as melanoma cells do, so it does not restrict the application of the model, either. The only crucial difference between the adhesion and the migration experiments is that the latter lasts much longer than the former for TCs captured on the substrate to migrate through the monolayer.

The number of migrated TCs per unit time and area, denoted by $\hat{n}_M$, is assumed to be directly proportional to N_{PT}:

$$\hat{n}_M = \xi N_{PT}, \tag{22}$$

where ξ is a coefficient depending on shear rate and viscosity. The experiments done by Liang et al. (6) show that a dynamic balance between aggregation and breakage takes several minutes once an experiment begins. In this equilibrium state, N_{PT} keeps constant. However,the experiments on TC migration lasted for 4 hours (2), thus

$$n_M = \int_{t=0}^{t=t_0} \hat{n}_M dt \approx \xi N_{PT}\big|_{t=\infty} t_0 = \xi t_0 \frac{BF}{\lambda_1 \lambda_2}, \tag{23}$$

So, n_M is directly proportional to $\frac{BF}{\lambda_1\lambda_2}$ at constant shear rate and viscosity. $\frac{BF}{\lambda_1\lambda_2}$ can be calculated by

$$\frac{BF}{\lambda_1\lambda_2} = \frac{BF}{AD-BC} = \frac{k_{PE}N_E^0}{xk_{PE}+y}, \tag{24}$$

where

$$x = \alpha \frac{b_{PT}+b_{PT-E}}{k_{PT}} + \beta, \tag{25}$$

$$y = \frac{b_{PT}+b_{PT-E}}{k_{PT}}\left(b_{PE}+k_{PT}\right) - b_{PT}, \tag{26}$$

α and β are functions of shear rate and viscosity unaffected by C_T or C_P, so x and y are only influenced by C_T. Thus, if C_T remains constant but increases n times, the ratio η of the number of migrated TCs at the current C_P to that at the original C_P becomes

$$\eta = \frac{\dfrac{k_{PE}(n)N_E^0}{xk_{PE}(n)+y}}{\dfrac{k_{PE}(1)N_E^0}{xk_{PE}(1)+y}} = \frac{n\left(xk_{PE}(1)+y\right)}{xnk_{PE}(1)+y}, \tag{27}$$

where $k_{PE}(1)$ denotes the k_{PE} when C_P is at its original value (the lowest concentration of PMNs adopted during experiments (2)) and $k_{PE}(n)$ denotes the k_{PE} when C_P increases n times.

Experiment results in Ref. (2) show that the migrated TCs increase by 92% when β_2 is doubled, but the migrated TCs only increase by 32% in existence of Interleukin-8 (IL-8). (IL-8 is a substance belonging to the superfamily of CXC chemokines and can promote the expression of Mac-1, a kind of β_2 integrins on PMNs, so it can enhance the tethering of PMNs to the monolayer.) Based on these results, the total number of migrated TCs in an experiment under various C_P is predicted, as shown by Fig. 9. It is found that the increase of the number of migrated TCs with C_P when IL-8 is added is not as much as that without it. To explain this result, let us consider n_M in a different way,

$$n_M \propto N_{PT}\big|_{t=\infty} = \frac{k_{PT}}{b_{PT}+b_{PT-E}} N_P\big|_{t=\infty}. \tag{28}$$

According to Eq. (28), the number of migrated TCs is proportional to the number of tethered PMNs on the monolayer at equilibrium. Physiologically, without IL-8, the PMNs are sparsely distributed on the monolayer. When IL-8 is added, the PMNs on the monolayer increase greatly. Since the maximum number of PMNs adhering to the monolayer is finite, tethered PMNs in

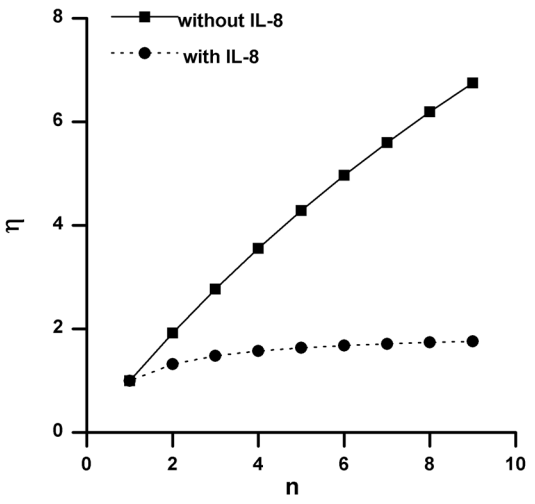

Figure 9. Predictions of the number of migrated TCs under different C_P. When IL-8 is added, η is smaller than that without IL-8 when n is greater than one.

equilibrium in the presence of IL-8 will not increase as much as that without IL-8 when C_P increases, and neither will the migrated TCs.

Conclusion

The current study provides a model to explain the previous experiments on cell adhesion in a parallel plate flow chamber (6). The model includes two population balance equations for the number of tethered PMN monomers and that of PMN-TC doublets on the EC monolayer, respectively. Based on analytical solutions of these equations, the curve fitting about aggregation percentage gives best-fit values of parameters in the model at different shear rates and viscosities, two of which, k_{PT} and $b_{PT}+b_{PT-E}$, are discussed. The results reveal that increase of shear rate and viscosity will prevent the formation and promote the breakage of PMN-TC doublets. The analysis on f_{PT} suggests that high viscosities or shear rates will make it difficult for moving TCs to collide with tethered PMNs unless the shear rate is large enough. The averaged encounter duration is influenced by viscosity rather than shear rate alone. Finally, the influence of the concentrations of PMNs and TCs in a flow on migration of TCs is analyzed. The conclusion is that the increase of the number of migrated TCs with C_P obviously depends on IL-8, and it will approach a constant rapidly if IL-8 is added.

Acknowledgements

This work was supported by the NSFC (21035004).

References

1. Slattery, M.J. and Dong, C., Neutrophils influence melanoma adhesion and migration under flow conditions. Int J Cancer, 2003, **106**:713–722. doi: 10.1002/ijc.11297

2. Slattery, M.J., Liang, S. and Dong, C., Distinct role of hydrodynamic shear in PMN-facilitated melanoma cell extravasation. Am J Physiol, 2005, **288(4)**: C831–C839. doi: 10.1152/ajpcell.00439.2004

3. Starkey, J.R., Liggitt, H.D., Jones, W. and Hosick, H.L., Influence of migratory blood cells on the attachment of tumor cells to vascular endothelium. Int J Cancer, 1984, 34:535–543. doi: 10.1002/ijc.2910340417

4. Welch, D.R., Schissel, D.J., Howrey, R.P. and Aeed, P.A., Tumor-elicited polymorphonuclear cells, in contrast to ‘‘normal’’ circulating polymorphonuclear cells, stimulate invasive and metastatic potentials of rat mammary adenocardinoma cells. Proc Natl Acad Sci U S A, 1989, **86**:5859–5863. doi: 10.1073/pnas.86.15.5859

5. Wu, Q., Wang, J., Condron, C., Bouchier-Hayer, D. and Redmond, H.P., Human neutrophils facilitate tumor cell transendothelial migration. Am J Phsyiol Cell Physiol, 2001, **280**:814–822. doi:

6. Liang, S., Slattery, M.J. and Dong, C., Shear stress and shear rate differentially affect the multi-step process of leukocyte-facilitated melanoma adhesion. Exp Cell Res, 2005, **310**:282–292. doi: 10.1016/j.yexcr.2005.07.028

7. Liang, S., Slattery, M.J., Wagner, D., Simon, S.I. and Dong C., Hydrodynamic shear rate regulates melanoma-leukocyte aggregations, melanoma adhesion to the endothelium and subsequent extravasation. Ann Biomed Eng, 2008, **36**:661–671. doi: 10.1007/s10439-008-9445-8

8. Liang, S., Hoskins, M. and Dong, C., Tumor cell extravasation mediated by leukocyte adhesion is shear ratedependent on IL-8 signaling. Mol Cell Biomech, 2009, **7**:77–91. doi:

9. Dong, C., Adhesion and signaling of tumor cells to leukocytes and endothelium in cancer metastasis. In: Cellular and biomolecular mechanics and mechanobiology, Amit, G. (ed.), Springer, 2011, pp. 477-521. doi: 10.1007/8415_2010_21

10. Liang, S., Fu, C., Wagner, D., Guo, H., Zhan, D., Dong, C. and Long, M., 2D kinetics of b2 integrin-ICAM-1 bindings between neutrophils and melanoma cells. Am J Physiol, 2008, **294**:743–753. doi: 10.1152/ajpcell.00250.2007

11. Long, M., Goldsmith, H.L., Tees, D.F. and Zhu, C., Probabilistic modeling of shear-induced formation and breakage of doublets cross-linked by receptor–ligand bonds. Biophys J, 1999, **76**:1112–1128. doi: 10.1016/S0006-3495(99)77276-0

12. Neelamegham, S., Taylor, A.D., Hellums, J.D., Dembo, M., Smith, C.W. and Simon, S.I., Modeling the reversible kinetics of neutrophil aggregation under hydrodynamic shear. Biophys J, 1997, **72**: 1527-1540. doi: 10.1016/S0006-3495(97)78801-5

13. Huang, P.Y. and Hellums, J.D., Aggregation and disaggregation kinetics of human blood platelets: Part I. Development and validation of a population balance method. Biophys J, 1993, **65**:334–343. doi: 10.1016/S0006-3495(93)81078-6

14. Belval, T.K. and Hellums, J.D., Analysis of shear-induced platelet aggregation with population balance mathematics. Biophys J, 1986, **50**:479–487. doi: 10.1016/S0006-3495(86)83485-3

15. Smoluchowski, M., Versuch einer mathematischen Theorie der Koagulations-kinetik kolloider Lösungen. Z Phys Chem, 1917, **92**:129 –188. doi:

16. Aldous, D.J., Deterministic and stochastic models for coalescence (aggregation and coagulation): a review of the Mean-Field Theory for Probabilities. Bernoulli, 1999, **5**:3–48. doi:

17. Wang, J., Slattery, M.J., Hoskins, M., Liang, S., Dong, C. and Du, Q., Monte Carlo simulation of heterotypic cell aggregation in nonlinear shear flow. Math Biosci Eng, 2006, **3**:683–696. doi:

18. Ma, Y., Wang, J., Liang, S., Dong, C. and Du, Q., Application of population dynamics to study heterotypic cell aggregations in the near-wall region of a shear flow. Cell Mol Bioeng, 2010, **3**: 3-19. doi: 10.1007/s12195-010-0114-2

19. Fu, C., Tong, C., Dong, C. and Long, M., Modeling of cell aggregation dynamics governed by receptor-ligand binding under shear flow. Cell Mol Bioeng, 2011, **4**: 427-441. doi: 10.1007/s12195-011-0167-x

20. Bartok, W., and Mason, S., Particle motions in sheared suspen-

sions: V. Rigid rods and collision doublets of spheres. J Colloid Interf Sci, 1957, **12**: 243–262. doi: 10.1016/0095-8522(57)90010-7
21. Wei, J., Lee and W., Krambeck, F.J., Catalyst attrition and deactivation in fluid catalytic cracking system. Chem Eng Sci, 1977, **32**:1211-1218. doi: 10.1016/0009-2509(77)80054-7
22. Pandya, J.D. and Spielman, L.A., Floc breakage in agitated suspensions: effect of agitation rate. Chem Eng Sci, 1983, **38**:1983-1992. doi: 10.1016/0009-2509(83)80102-X
23. Spicer, P.T. and Pratsinis, S.T., Coagulation and fragmentation: universal steady-state particle-size distribution. AIChE J, 1996, **42**:1612-1620. doi: 10.1002/aic.690420612
24. Serra, T. and Casamitjana, X., Effect of the shear and volume fraction on the aggregation and breakup of particles. AIChE J, 1998, **44**: 1724-1730. doi: 10.1002/aic.690440803
25. Chesla, S., Selvaraj, P., and Zhu, C., Measuring two-dimensional receptor–ligand binding kinetics by micropipette. Biophys J, 1998, **75**:1553–1572. doi: 10.1016/S0006-3495(98)74074-3
26. Bell, G.I., Models for the specific adhesion of cells to cells. Science, 1978, **200**:618–627. doi: 10.1126/science.347575